

Sensor Fault Detection for Salient PMSM based on Parity-Space Residual Generation and Robust Exact Differentiation

Benjamin Jahn^{*,**} Michael Brückner^{**} Stanislav Gerber^{**}
Yuri A.W. Shardt^{*}

^{*} Department of Automation Engineering, Technical University of Ilmenau, D-98684 Ilmenau, Germany

^{**} Nidec driveXpert GmbH, D-98693 Ilmenau, Germany

Abstract: An online model-based fault detection and isolation method for salient permanent magnet synchronous motors is proposed using the parity-space approach. Given the polynomial model equations, Buchberger's algorithm is used to eliminate the unknown variables (e.g. states, unmeasured inputs) resulting in analytic redundancy relations for residual generation. Furthermore, in order to obtain the derivatives of measured signals needed by such a residual generator, robust exact differentiators are used. The fault detection and isolation method is demonstrated using simulation of various fault scenarios for a speed controlled salient motor showing the effectiveness of the presented approach.

Copyright © 2020 The Authors. This is an open access article under the CC BY-NC-ND license (<http://creativecommons.org/licenses/by-nc-nd/4.0>)

Keywords: Permanent Magnet Synchronous Motor, Sensor Fault Detection, Analytic Redundancy Relations, Robust Exact Differentiators

1. INTRODUCTION

Due to their high efficiency and power density, permanent magnet synchronous motors (PMSM) are frequently used in various industrial fields. In almost all applications, detecting sensor errors affecting current or speed / position measurements improves safety and minimizes the environmental impact and economic losses. By implementing an online fault detection and isolation (FDI) method, the process can be monitored and unusual behavior can be identified and appropriate countermeasures taken.

Over the last decades, FDI has been the subject of intensive research for both linear and nonlinear systems leading to different types of methods (Chen et al., 2001; Ding, 2008). These methods can be broadly classified into two categories: data-driven FDI and model-based FDI. Unlike model-based methods, data-driven methods do not rely on accurate *a priori* model knowledge but on available historical data making them more suitable for large-scale systems in process engineering. Data-driven approaches range from multivariate statistical to machine learning approaches (Qin, 2012; Chen et al., 2016, 2017; Hua et al., 2018).

Within the model-based FDI methods, the parity-space based approach uses a set of analytic redundancy relations derived from the model equations that involve only known quantities and can be used for residual generation (Isidori et al., 2001; Blanke, 2015). The parity-space approach was first investigated for linear systems by Chow and Willsky (1984) and can be generalized to cover polynomial systems (Frank, 1990; Kinnaert, 2003). The elimination of unknown quantities can be performed using Buchberger's algorithm for finding a Groebner basis, which results in the

final residuals. In Comtet-Varga et al. (1999), a similar approach has been applied to induction motors. Other recent results on PMSM make use of different observer-based approaches (Foo et al., 2013; Kommuri et al., 2018).

In general, evaluation of the resulting residuals requires the derivatives of measured input and output quantities. This might be impractical since these derivatives are not directly available and numerical differentiation of noisy measured quantities is impractical.

Therefore, this paper will examine the application of robust exact differentiators, first introduced by Levant (1998, 2003), to the PMSM system in order to obtain a practical residual generator based on the found analytic redundancy relations.

This paper is structured as follows: in Section 2, model-based FDI in general, the parity-space based approach in particular and robust exact differentiators are shortly recapitulated. In Section 3, their combination in order to implement fault detection for polynomial systems is proposed. In Section 4, this combination is applied to the detection of sensor faults of a salient PMSM. For that purpose, suitable analytic redundancy relations are derived based on the standard dynamic model of a PMSM. Finally, the proposed sensor fault detection is demonstrated by means of simulation in Section 5.

2. BACKGROUND

The basic principle of model-based FDI is to compare the expected system behavior (by means of a model) with the actual one. In order to quantify the level of mismatch or discrepancy a set of residual signals is generated. Figure 1 shows the quantitative model-based FDI

approach involving two stages: diagnostic / residual signal generation and decision making or diagnostic classification (Chen et al., 2001). Such a residual signal has to satisfy specific properties given by Definition 1 such that their generation/construction is a non-trivial task especially for nonlinear systems. Many different approaches for residual generation have been proposed that can be divided into three categories: observer-based, parity-space based and parameter estimation/identification based approaches (Frank, 1990).

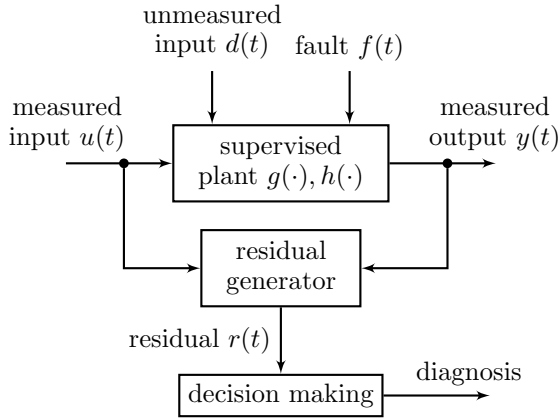


Fig. 1. Two stages of quantitative model-based FDI (after (Chen et al., 2001))

Definition 1. A residual is a signal that is zero when the system under diagnosis is free of faults, and nonzero when particular faults are present in the system. Additionally, a residual must be invariant to any unmeasured and therefore unknown input signals (e.g. disturbances) as their influence is not considered as a fault.

2.1 Parity-space based approach for polynomial nonlinear systems

The parity-space approach was first investigated for linear systems by Chow and Willsky (1984) and can be generalized to cover polynomial systems (Kinnaert, 2003; Isidori et al., 2001). The approach is based on analytic redundancy relations (ARR), which can be used for residual generation and subsequent FDI (Chen et al., 2001).

Consider the class of polynomial multiple-input multiple-output (MIMO) systems

$$\dot{x} = g(x, u, d, f) \quad (1a)$$

$$y = h(x, u, d, f) \quad (1b)$$

where $g : \mathbb{R}^n \times \mathbb{R}^p \times \mathbb{R}^{n_d} \times \mathbb{R}^{n_f} \rightarrow \mathbb{R}^n$ and $h : \mathbb{R}^n \times \mathbb{R}^p \times \mathbb{R}^{n_d} \times \mathbb{R}^{n_f} \rightarrow \mathbb{R}^q$ are polynomial functions of their arguments, i.e. x the state vector, u the vector of known inputs, d the vector of unknown inputs or disturbances and f the vector of faults. Further, consider the s_j successive time derivatives of the j^{th} output

$$Y_j^{(s_j)} = H_j(x, U^{(s_j)}, D^{(s_j)}, F^{(s_j)}) \quad (2)$$

where $Y_j^{(s_j)}$ is a vector consisting of y_j and its derivatives up to order s_j . The same notation applies to the measured and unmeasured inputs $U^{(s_j)}$, $D^{(s_j)}$ and faults $F^{(s_j)}$ as well

as their derivatives up to order s_j . The concatenation of this equation for all outputs leads to the following system of $\sum_j (s_j + 1)$ equations

$$Y = H(x, U^{(s)}, D^{(s)}, F^{(s)}) \quad (3)$$

where $s = \max_j s_j$ ¹. Since the states x and the unmeasured inputs d are not available, they need to be eliminated in order to get analytic redundancy relations that can be used for FDI. Elimination can be performed by finding a Groebner basis using Buchberger's algorithm (Buchberger, 1985; Cox et al., 1992). Alternatives for computing Groebner bases are p -adic and modular methods that have been successful in limiting intermediate coefficient growth, which is a prominent challenge of Buchberger's algorithm (Arnold, 2003). Another constructive method to eliminate variables of a given set of polynomial equations can be found in Ritt's algorithm (Ritt, 1950), which is also used in nonlinear system identification (Ljung and Glad, 1994).

This elimination results in a set of polynomials (ARR)²

$$P(Y, U, F) = 0 \quad (4)$$

which can then be decomposed due to their polynomial structure as

$$P(Y, U, F) = P_r(Y, U) + P_f(Y, U, F) = 0 \quad (5)$$

where $P_f(Y, U, F)$ equals zero in faultless operation, if decomposition has been made such that each polynomial of $P_f(Y, U, F)$ is of degree of at least one with respect to any entry of F . Finally, the resulting polynomials $P_r(Y, U)$ can be interpreted as the parity / residual signal used for fault detection (to achieve isolation, structured residuals have to be calculated), that is

$$r(t) = P_r(Y(t), U(t)) \quad (6)$$

However, the fact that these expressions consist of the derivatives of the measured input and output constitutes the main drawback of this method for residual generation. As it is often the case, in practice, these derivatives are not accessible using numerical differentiation due to measurement noise. This problem becomes worse as the order of derivatives needed increases. Most often it is proposed to generate a filtered version of the residual signal; thereby avoiding the need for the derivatives. Here another method to evaluate (6) for residual generation is used in order to deal with the noise.

2.2 Differentiation using robust exact differentiators

In Levant (2003), an arbitrary order differentiator that is exact on a large class of signals and robust with respect to small amounts of noise of any frequency is proposed. In order to estimate the successive derivatives $x^{(i)}(t)$, $i = 1, \dots, n-1$ of a measured base signal $x(t)$, it uses a high-order sliding mode observer based on the following signal model ($x_n = x^{(n-1)}$)

$$\dot{x} = x_1, \quad \dot{x}_1 = x_2, \quad \dot{x}_2 = x_3 \quad \dots \quad \dot{x}_{n-1} = x^{(n)}(t) \quad (7)$$

¹ depending on the relative degree of u , d and f the maximum order of the derivatives needed might be smaller than s

² for the sake of convenience, the maximum order will be omitted in the following, e.g. $U^{(s)} = U$

with a known upper bound for the Lipschitz-constant $L > 0$ of its n -th derivative. The $(n - 1)$ -th order differentiator is then

$$\dot{\hat{x}}_i = -k_i [\hat{x}_1 - x_1]^{\frac{n-i}{n}} + \hat{x}_{i+1}, \quad i = 1, \dots, n-1 \quad (8a)$$

$$\dot{\hat{x}}_n = -k_n \operatorname{sgn}(\hat{x}_1 - x_1) \quad (8b)$$

where $[x]^p = |x|^p \operatorname{sgn}(x)$. To guarantee finite-time exact convergence in the absence of noise, k_1, \dots, k_n need to be chosen with respect to L , as shown by Levant (2003). In applications requiring a wide range of operation, it may be necessary for L to be very large resulting in high observer gains. In the presence of considerable measurement noise, this degrades the performance of the differentiator. To tackle this problem, filtering differentiators which are capable of both rejecting large noise and exactly differentiating smooth signals have been proposed recently (Levant and Livne, 2019). Another extension given by variable gain exact differentiators (Levant, 2006, 2014) deals with the case where the n -th derivative is not uniformly bounded, but its bound is given by a time-varying function. Although other variants exist, the approach chosen in the paper was selected due to its simplicity.

3. PROPOSED RESIDUAL GENERATION

Robust exact differentiators as presented before can be used to generate all needed derivatives in the ARR (see Equation (6)) to give an exact, robust and nonlinear filtered residual signal. Figure 2 shows the proposed residual generator

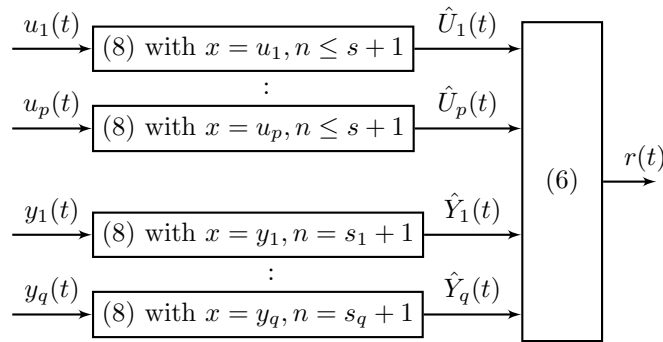


Fig. 2. Schematic of the proposed residual generator using robust exact differentiators for ARR evaluation

where $\hat{U}_1, \dots, \hat{U}_p$ are the estimates of every input and their needed derivatives and $\hat{Y}_1, \dots, \hat{Y}_p$ are the estimates of every output and their needed derivatives for evaluation of (6). Instead of using the unavailable derivatives for the evaluation of the ARR, estimates provided by multiple robust exact differentiators are used. Therefore, for each input signal a robust exact differentiator of order $n \leq s + 1$ (depending on the minimal relative degree of the input w.r.t. to each output) and for each output signal of order $n = s_j + 1$ is needed.

4. SENSOR FAULT DETECTION AND ISOLATION FOR PMSM

Given the importance of PMSM in industry, background information about PMSM will be provided in this section.

Then the proposed method will be applied to the PMSM system.

4.1 Permanent Magnet Synchronous Machines (PMSM)

All AC phase currents and voltages of three-phase synchronous machines are usually expressed in a rotor-fixed (rotating) coordinate system (the d/q -frame) using the Clarke and Park transformation. Figure 3 shows a rotating motor with angular position φ and the resulting projection of a sample stator current vector i_s onto the axes of the rotor-fixed d/q -frame.

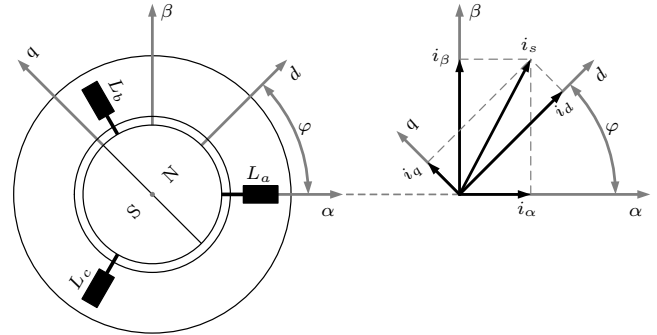


Fig. 3. Stator current expressed in rotor-fixed (rotating) d/q -frame using the Clarke and Park transformation

Using these transformations, the electrical dynamics of the PMSM is commonly described as (Schröder, 1995)

$$L_d \frac{d}{dt} i_d = -R i_d + p\omega L_q i_q + u_d \quad (9a)$$

$$L_q \frac{d}{dt} i_q = -R i_q - p\omega L_d i_d - p\omega \Psi + u_q \quad (9b)$$

where i_d, i_q and u_d, u_q represent the direct (in-phase) and quadrature components of the motor currents and voltages expressed in rotor-fixed coordinates and ω the angular velocity of the rotor. The strictly positive parameters L_d, L_q, R, Ψ and p are respectively the direct/quadrature inductivity, phase resistance, flux linkage of the permanent magnet and the number of pole pairs. In general, for a salient motor the direct component of the inductivity is smaller than the quadrature component, i.e. $L_d < L_q$.

The rotor shaft dynamics are determined using Newton's second law of motion as

$$J\dot{\omega} = -d\omega + \tau_m + \tau_d \quad (10)$$

while the torque produced by the PMSM equals $\tau_m = \frac{3p}{2}(\Psi + (L_d - L_q)i_d)i_q$. The parameters J and d are the rotor's moment of inertia and the viscous friction coefficient. The term τ_d represents any additional torque applied to the rotor shaft, e.g. the load torque. The state vector is composed of the motor's d/q -currents and the angular speed $x = [i_d, i_q, \omega]^T$.

Considering additive sensor faults f_d, f_q, f_ω , the output equations $y = [y_d, y_q, y_\omega]^T$ are given by

$$y_d = i_d + f_d \quad y_q = i_q + f_q \quad y_\omega = \omega + f_\omega \quad (11)$$

Remark. It is important to note that i_d and i_q are only computational quantities after Clarke and Park transformation of measured phase currents. A constant phase cur-

rent sensor fault will result in a combined sensor fault in f_d and f_q depending on the angular position of the motor.

4.2 Residual generation

Taking the derivative of the output Equation (11) and substitution of the dynamic Equations (9) and (10) gives

$$L_d \dot{y}_d = -Ri_d + p\omega L_q i_q + u_d + L_d \dot{f}_d \quad (12a)$$

$$L_q \dot{y}_q = -Ri_q - p\omega L_d i_d - p\omega \Psi + u_q + L_q \dot{f}_q \quad (12b)$$

$$J \dot{y}_\omega = -d\omega + J \dot{f}_\omega + \tau_d + \frac{3p}{2}(\Psi + (L_d - L_q)i_d)i_q \quad (12c)$$

Together with the output equations they constitute a set of 6 equations. Following the procedure from Subsection 2.1, elimination of the unknown states i_d, i_q, ω can be achieved by simply substituting the output equations. To eliminate the unmeasured input τ_d , the approach of finding a Groebner basis using the Buchberger's algorithm (Buchberger, 1985; Cox et al., 1992) for a set of polynomial equations is used as in Guernez et al. (1997). The symbolic computations have been performed using SymPy, a library for the programming language Python for symbolic computations. The derived set of polynomial expressions according to Equation (4) is given in Appendix A.

The next step is to decompose this Equation (4) into P_r and P_f , while P_f contains all terms depending on the faults f_d, f_q, f_ω and their derivatives. This guarantees that P_f equals zero in the faultless case, i.e. $f_d, f_q, f_\omega \equiv 0$. Finally, the residual signal needed for fault detection $P_r(y_d, \dot{y}_d, y_q, \dot{y}_q, y_\omega, u_d, u_q) = [r_1, r_2, r_3]^T$ is given by

$$r_1 = +L_d^2 \dot{y}_d y_d + L_d \Psi \dot{y}_d + L_d R y_d^2 - L_d u_d y_d + L_q^2 \dot{y}_q y_q + L_q R y_q^2 - L_q u_q y_q + \Psi R y_d - \Psi u_d \quad (13a)$$

$$r_2 = -L_d L_q p^2 y_d y_\omega^2 - L_d R \dot{y}_d - L_q^2 \dot{y}_q p y_\omega - L_q \Psi p^2 y_\omega^2 + L_q p u_q y_\omega - R^2 y_d + R u_d \quad (13b)$$

$$r_3 = +L_d^2 \dot{y}_d p y_\omega - L_d L_q p^2 y_q y_\omega^2 - L_d p u_d y_\omega - L_q R \dot{y}_q - \Psi R p y_\omega - R^2 y_q + R u_q \quad (13c)$$

As explained in Section 2, a robust exact differentiator can be used to estimate the derivatives of the system's outputs y_d and y_q needed for the residual signals in Equation (13). Since only first-order derivatives are needed, the estimator reduces to a classical super-twisting sliding mode (second order) observer as introduced by Levant (1998)

$$\dot{\hat{x}} = -k_1 |\hat{x} - x|^{1/2} \text{sgn}(\hat{x} - x) + v \quad (14a)$$

$$v = -k_2 \text{sgn}(\hat{x} - x) \quad (14b)$$

As proposed, these estimates of the derivatives of the system's outputs y_d and y_q are used to evaluate the ARR of the PMSM given by Equation (13) so as to complete the residual generator design.

4.3 Residual evaluation and decision making

In real application, the residual signal will always deviate from zero due to measurement noise and modeling errors. Therefore, in terms of residual evaluation, the simplest method is to introduce a threshold below which the residual is considered to be inactive. Such a threshold

might be determined by conducting simulations with noisy measurements and/or actual plant measurements.

Since the diagnosis system should not only detect faults but also isolate them, the influence of individual faults on the residual signal needs to be studied. Further inspections of Equation (A.1) for the case of constant faults shows the influence of individual faults on the residual signals as shown in Table 1. For example, assume that residuals r_1 and r_3 are active (i.e. above the relevant threshold) while r_2 is inactive. Then the second column of Table 1 tells us that fault f_q must have occurred. It is clear that only individually occurring faults can be isolated. As soon as two or more faults occur, they cannot be distinguished by residual evaluation using the proposed residuals. Unfortunately, as it was stated in the last remark, a phase current sensor fault results in a combined sensor fault in f_d and f_q . As all three residuals are active in such a case, this cannot be distinguished from an additional speed sensor fault occurring. Therefore, if all three residuals are active, one cannot decide whether it is a phase current sensor fault only or also an additional speed sensor fault.

Table 1. Effect of faults on each individual residual signal (coding table)

	f_d	f_q	f_ω
r_1	x	x	
r_2	x		x
r_3		x	x

5. SIMULATION STUDIES

The proposed FDI method is simulated for a speed controlled salient PMSM with parameters given in Table 2. The control strategy follows a classical field-orientated vector control law with current set points chosen according to the motor's maximum-torque-per-ampere (MTPA) curve.

The control and FDI algorithms are simulated to run at a fixed sampling rate of $T_s = 0.1$ ms while the plant is modeled continuously and numerically solved using the Dormand-Prince method (ode45) with variable step size. The gains of the robust exact differentiators used to estimate the derivatives of y_d and y_q have been set to $k_1 = 50$, $k_2 = 75$. For this simulation study, it is assumed that the speed can be measured and does not need to be estimated based on position measurements. Gaussian white noise with standard deviations $\sigma_i = 0.5$ A and $\sigma_\omega = 1.5$ rpm (min^{-1}) is added to the d/q -current and speed sensors. At the beginning of the simulation, the motor is accelerated to a target speed of 1800 rpm (min^{-1}). At $t = 2$ s, an external load torque of 0.5 N m is applied to

Table 2. Parameters of PMSM

parameter	value
phase resistance - R	9.25 m Ω
d -axis inductance - L_d	0.895 μ H
q -axis inductance - L_q	1.044 μ H
flux linkage - Ψ	4.8751 mWb
pole pairs - p	5
rotor inertia - J	0.0113 N m s 2
friction coefficient - d	0.002 N m s rad $^{-1}$

the motor such that about 45 A phase current is required in steady state. During the interval $t = [4, 5)$ s, sensor fault $f_d = 4$ A is active; $t = [5, 6)$ s, sensor fault $f_q = 4$ A is active; and $t = [6, 7)$ s, sensor fault $f_\omega = 250$ rpm (min^{-1}) is active.

Figure 4 shows the simulation results. Until $t = 4$ s the residuals are close to zero and only the effect of measurement noise can be observed. Note that the load change at $t = 2$ s has no influence on the residuals, as expected. Introduction of a suitable threshold for each residual (above measurement noise and modeling error band and below active fault output) allows the following residual evaluation and decision to be made based on the effects of the faults on each residual (see Table 1)

- for $t = [4, 5)$ s : $\mathcal{R} = \{r_1, r_2\} \rightarrow f_d$ detected
- for $t = [5, 6)$ s : $\mathcal{R} = \{r_1, r_3\} \rightarrow f_q$ detected
- for $t = [6, 7)$ s : $\mathcal{R} = \{r_2, r_3\} \rightarrow f_\omega$ detected

with $\mathcal{R} = \{r_i \mid \forall i \in \{1, 2, 3\} : r_i \text{ active}\}$ being the set of active residuals.

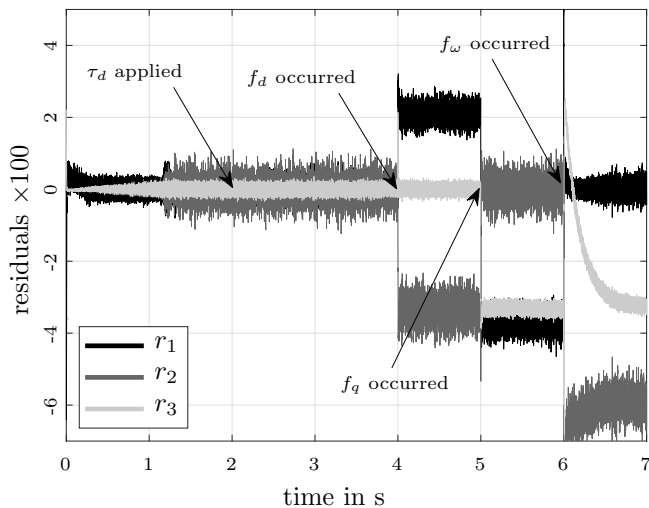


Fig. 4. Residual signals during motor run and sensor faults

The transient behavior of r_3 in case of a speed sensor fault f_ω needs to be highlighted at this point. The reason for this can be found in the last line of Equation (A.1c), where the influence of f_ω on the third ARR depends on the speed output y_ω . Since the simulated PMSM is speed controlled, the controller slowly compensates for the output disturbance resulting in transient behavior of the angular velocity which can be seen in the third residual. Apart from that, the residual signals react immediately to the fault actions due to the use of robust exact differentiators. This enables fast fault detection and reaction.

6. CONCLUSION AND FUTURE WORK

This paper has presented the design of a residual generator for sensor fault detection of PMSM. The main contribution is to combine ARR evaluation based on the parity-space based approach with robust exact differentiators in order to derive an exact, robust and nonlinear filtered residual signal. This result has been applied to a model of a PMSM. For this purpose three analytic redundancy relations, which are robust against unknown load torques,

have been obtained by elimination according to Buchberger's algorithm for finding a Groebner basis of polynomials. Simulation results show that speed and current sensor faults can be detected. A weakness of the proposed approach is that it cannot distinguish between the cases of phase current sensor faults only and an additional speed sensor fault, since both cases have the same residual signature. However, in both cases, the current measurements are defective, which normally makes the control of the PMSM unsafe and uneconomic.

As next step, the proposed method is to be applied to an actual PMSM in order to evaluate its performance under real conditions. Furthermore, since, in real applications, measurements are normally provided by phase current sensors and position sensors, the influence of faults on these measurements needs to be investigated.

ACKNOWLEDGEMENTS

The authors acknowledge the financial and technical support by Nidec driveXpert GmbH. The authors thank Dr. Sandro Purfürst for his planning and coordination work for this collaboration, and Bastian Schindler for providing a figure of the PMSM and its coordinate transformations.

REFERENCES

- E. A. Arnold. Modular algorithms for computing Gröbner bases. *Journal of Symbolic Computation*, 35(4):403 – 419, 2003. ISSN 0747-7171. doi: 10.1016/S0747-7171(02)00140-2.
- Mogens Blanke. *Diagnosis and fault-tolerant control*. Springer, Heidelberg, 2015. ISBN 978-3-662-47942-1.
- B. Buchberger. Gröbner bases: An algorithmic method in polynomial ideal theory. In N. K. Bose, editor, *Multidimensional Systems Theory and Applications*, pages 89–127. Springer Netherlands, Dordrecht, 1985. ISBN 978-94-017-0275-1. doi: 10.1007/978-94-017-0275-1_4.
- J. Chen, P. M. Frank, M. Kinnaert, J. Lunze, and R. J. Patton. Fault detection and isolation. In Karl Åström, Pedro Albertos, Mogens Blanke, Alberto Isidori, Walter Schaufelberger, and Ricardo Sanz, editors, *Control of Complex Systems*, pages 191–207. Springer London, London, 2001. ISBN 978-1-4471-0349-3. doi: 10.1007/978-1-4471-0349-3_9.
- Zhiwen Chen, Steven X. Ding, Kai Zhang, Zhebin Li, and Zhikun Hu. Canonical correlation analysis-based fault detection methods with application to alumina evaporation process. *Control Engineering Practice*, 46:51 – 58, 2016. ISSN 0967-0661. doi: 10.1016/j.conengprac.2015.10.006.
- Zhiwen Chen, Kai Zhang, Yuri A.W. Shardt, Steven X. Ding, Xu Yang, Chunhua Yang, and Tao Peng. Comparison of two basic statistics for fault detection and process monitoring. *IFAC-PapersOnLine*, 50(1):14776 – 14781, 2017. ISSN 2405-8963. doi: 10.1016/j.ifacol.2017.08.2586. 20th IFAC World Congress.
- E. Chow and A. Willsky. Analytical redundancy and the design of robust failure detection systems. *IEEE Transactions on Automatic Control*, 29(7):603–614, July 1984. ISSN 0018-9286. doi: 10.1109/TAC.1984.1103593.
- G. Comtet-Varga, C. Christophe, V. Cocquempot, and M. Staroswiecki. F.D.I. for the induction motor

- using elimination theory. In *1999 European Control Conference (ECC)*, pages 4473–4478, Aug 1999. doi: 10.23919/ECC.1999.7100039.
- David A. Cox, John Little, and Donal O’Shea. *Ideals, Varieties, and Algorithms: an introduction to computational algebraic geometry and commutative algebra*. Springer, New York, 1992.
- Steven X. Ding. *Model-based Fault Diagnosis Techniques: Design Schemes, Algorithms, and Tools*. Springer Publishing Company, Incorporated, 1st edition, 2008. ISBN 9783540763031.
- G. H. B. Foo, X. Zhang, and D. M. Vilathgamuwa. A sensor fault detection and isolation method in interior permanent-magnet synchronous motor drives based on an extended kalman filter. *IEEE Transactions on Industrial Electronics*, 60(8):3485–3495, 2013.
- Paul M. Frank. Fault diagnosis in dynamic systems using analytical and knowledge-based redundancy: A survey and some new results. *Automatica*, 26(3):459 – 474, 1990. ISSN 0005-1098. doi: 10.1016/0005-1098(90)90018-D.
- C. Guernez, J. Ph. Cassar, and M. Staroswiecki. Extension of parity space to non linear polynomial dynamic systems. *IFAC Proceedings Volumes*, 30(18):857 – 862, 1997. ISSN 1474-6670. doi: 10.1016/S1474-6670(17)42507-9.
- Changsheng Hua, Steven X. Ding, and Yuri A.W. Shardt. A new method for fault tolerant control through Q-learning. *IFAC-PapersOnLine*, 51(24):38 – 45, 2018. ISSN 2405-8963. doi: 10.1016/j.ifacol.2018.09.526. 10th IFAC Symposium on Fault Detection, Supervision and Safety for Technical Processes SAFEPROCESS 2018.
- A. Isidori, M. Kinnaert, V. Cocquemot, C. De Persis, P. M. Frank, and D. N. Shields. Residual generation for FDI in non-linear systems. In Karl Åström, Pedro Albertos, Mogens Blanke, Alberto Isidori, Walter Schaufelberger, and Ricardo Sanz, editors, *Control of Complex Systems*, pages 209–227. Springer London, London, 2001. ISBN 978-1-4471-0349-3. doi: 10.1007/978-1-4471-0349-3_10.
- M. Kinnaert. Fault diagnosis based on analytical models for linear and nonlinear systems - a tutorial. *IFAC Proceedings Volumes*, 36(5):37 – 50, 2003. ISSN 1474-6670. doi: 10.1016/S1474-6670(17)36468-6. 5th IFAC Symposium on Fault Detection, Supervision and Safety of Technical Processes 2003, Washington DC, 9-11 June 1997.
- S. K. Kommuri, S. B. Lee, and K. C. Veluvolu. Robust sensors-fault-tolerance with sliding mode estimation and control for pmsm drives. *IEEE/ASME Transactions on Mechatronics*, 23(1):17–28, 2018.
- A. Levant. Robust exact differentiation via sliding mode technique. *Automatica*, 34(3):379–384, March 1998. ISSN 0005-1098. doi: 10.1016/S0005-1098(97)00209-4.
- A. Levant. Higher-order sliding modes, differentiation and output-feedback control. *International Journal of Control*, 76(9-10):924–941, 2003. doi: 10.1080/0020717031000099029.
- A. Levant. Exact differentiation of signals with unbounded higher derivatives. In *Proceedings of the 45th IEEE Conference on Decision and Control*, pages 5585–5590, 2006.
- A. Levant. Globally convergent fast exact differentiator with variable gains. In *2014 European Control Conference (ECC)*, pages 2925–2930, 2014.
- A. Levant and M. Livne. Robust exact filtering differentiators. *European Journal of Control*, 2019. ISSN 0947-3580. doi: 10.1016/j.ejcon.2019.08.006.
- Lennart Ljung and Torkel Glad. On global identifiability for arbitrary model parametrizations. *Automatica*, 30(2):265 – 276, 1994. ISSN 0005-1098. doi: 10.1016/0005-1098(94)90029-9.
- S. Joe Qin. Survey on data-driven industrial process monitoring and diagnosis. *Annual Reviews in Control*, 36(2):220 – 234, 2012. ISSN 1367-5788. doi: 10.1016/j.arcontrol.2012.09.004.
- J. F. Ritt. *Differential Algebra*. Colloquium publications. American Mathematical Society, 1950. ISBN 9780821846384.
- D. Schröder. *Elektrische Antriebe - Regelung von Antriebssystemen [Electrical drives - control of drive systems]*. Springer Berlin Heidelberg, 1995. ISBN 9783642300950.

Appendix A. COMPUTED GROEBNER BASIS

The elimination of the external load τ_d has been achieved by Buchberger’s algorithm for finding a Groebner basis. The vector of polynomials $P = [P_1, P_2, P_3]^T$ given by Equation (A.1) depends only on the outputs y_d, y_q, y_ω , the output derivatives \dot{y}_d, \dot{y}_q , the inputs u_d, u_q , the fault signals f_d, f_q, f_ω and the fault signal derivatives \dot{f}_d, \dot{f}_q .

$$\begin{aligned}
 P_1 = & -L_d^2 \dot{f}_d y_d + L_d^2 \dot{y}_d y_d - L_d \Psi \dot{f}_d + L_d \Psi \dot{y}_d + L_d R y_d^2 \\
 & + L_d R f_d^2 - L_d u_d y_d - L_d^2 \dot{f}_q y_q + L_d^2 \dot{y}_q y_q + L_d R y_q^2 \\
 & + L_d R f_q^2 - L_d u_q y_q + \Psi R y_d - \Psi u_d \\
 & - (-L_d^2 \dot{f}_d + L_d^2 \dot{y}_d + 2L_d R y_d - L_d u_d + \Psi R) f_d \\
 & + L_q (L_q \dot{f}_q - L_q \dot{y}_q - 2R y_q + u_q) f_q \quad (A.1a)
 \end{aligned}$$

$$\begin{aligned}
 P_2 = & -L_d L_q p^2 y_d y_\omega^2 - L_d L_q p^2 (2y_\omega - f_\omega) f_d f_\omega \\
 & + L_d R \dot{f}_d - L_d R \dot{y}_d + L_d^2 \dot{f}_q p y_\omega - L_d^2 \dot{y}_q p y_\omega \\
 & - L_q \Psi p^2 y_\omega^2 - L_q p^2 (L_d y_d + \Psi) f_\omega^2 + L_q p u_q y_\omega \\
 & + L_q p (2L_d p y_d y_\omega - L_q \dot{f}_q + L_q \dot{y}_q + 2\Psi p y_\omega - u_q) f_\omega \\
 & - R^2 y_d + R u_d + (L_d L_q p^2 y_\omega^2 + R^2) f_d \quad (A.1b)
 \end{aligned}$$

$$\begin{aligned}
 P_3 = & -L_d^2 \dot{f}_d p y_\omega + L_d^2 \dot{y}_d p y_\omega - L_d L_q p^2 y_q y_\omega^2 - L_d p u_d y_\omega \\
 & - L_d L_q p^2 (y_q f_\omega + 2y_\omega f_q - f_q f_\omega) f_\omega + L_q R \dot{f}_q \\
 & - L_q R \dot{y}_q - \Psi R p y_\omega - R^2 y_q + R u_q \\
 & + (L_d L_q p^2 y_\omega^2 + R^2) f_q \\
 & + p (L_d^2 \dot{f}_d - L_d^2 \dot{y}_d + 2L_d L_q p y_q y_\omega + L_d u_d + \Psi R) f_\omega \quad (A.1c)
 \end{aligned}$$